

Electric feed systems for liquid propellant rockets

P.A. Pavlov Rachov,* H. Tacca[†]

Universidad de Buenos Aires

Buenos Aires, Argentina

D. Lentini[‡]

Sapienza Università di Roma

I-00184 Roma RM, Italy

November 19, 2012

Abstract

Liquid propellant rocket feed systems based on electric pumps are compared to the more classical pressure-gas and turbopump systems. The design parameters entering in the definition of the system mass are highlighted, and a careful choice of the figures of merit is performed, in particular for the electric motors and batteries. Indeed, recent developments, taking into account new electric motors based

*Undergraduate Electronic Engineering Student, Laboratorio de Control de Accionamientos, Tracción y Potencia, Departamento de Electrónica, F.I.U.B.A., Paseo Colón 850, e-mail rachov@gmail.com.

[†]Associate Professor, Laboratorio de Control de Accionamientos, Tracción y Potencia, Departamento de Electrónica, F.I.U.B.A., Paseo Colón 850, e-mail htacca@fi.uba.ar. Member AIAA.

[‡]Associate Professor, Dipartimento di Ingegneria Meccanica e Aerospaziale, Via Eudossiana 18, e-mail diego.lentini@uniroma1.it; corresponding author. Senior Member AIAA.

on rare earth permanent magnets (neodymium–iron–boron), and different lithium-based cells, show that the specific mass of the electric pump system can be reduced to such an extent to make the proposed system competitive not only with the pressure–gas system, but also with the turbopump one, at least for some applications such as small launchers and upper stage rockets. Further, electric motor and battery cell technologies currently under development could extend the proposed feed system convenience. Critical points related to electric pump systems are also discussed.

Nomenclature

C_1, C_2	constants defined by Eqs. (3,4)
D_1 through D_{12}	constants defined by Eqs. (22–30, 46–48)
E_e	electric energy
f, g, h	functions defined by Eqs. (2,49,32)
m	mass
\mathcal{M}	molar mass
O/F	oxidizer–to–fuel mass flow ratio
p	pressure
P	power
r	tank radius
R^0	universal gas constant
s	relative sensitivity of overall payload mass ratio
t_b	burning time
t_s	stay time
T	absolute temperature
V	volume
W/F	water–to–fuel mass flow ratio

$\alpha, \alpha_f, \alpha_o$	quantities defined by Eq. (6)
α', α_w	quantities defined by Eq. (10)
β_f	quantity defined by Eq. (8)
γ	specific heats ratio
δ_E, δ_P	battery energy and power densities
$\delta_{em}, \delta_{inv}$	electric motor and inverter power densities
δ_{pu}, δ_{tu}	pump and turbine power densities
$\Delta h_{tu,s}$	isentropic turbine enthalpy jump
η	efficiency
κ_b	safety factor for batteries
κ_g	safety factor for pressurizing gas mass
κ_{gg}	safety factor for gas generator wall thickness
$\kappa_{p1}, \kappa_{p2}, \kappa_{p3}$	pressure ratios defined by Eqs. (5,31,9)
κ_t	safety factor for tank wall thickness
κ_u	ratio of tank volume to propellant volume
λ	overall payload mass ratio
μ_{ep}	electric pump specific mass
ρ	density
σ_t	stress admitted by tank wall material
τ	tank wall thickness

Subscripts

<i>b</i>	batteries
<i>c</i>	combustion chamber
<i>e</i>	electric
<i>em</i>	electric motor
<i>ep</i>	electric pumps
<i>eps</i>	electric pump system
<i>f</i>	fuel
<i>fs</i>	feed system
<i>g</i>	pressurizing gas
<i>gg</i>	gas generator
<i>in</i>	inlet
<i>inv</i>	inverter
<i>m</i>	material
<i>min</i>	minimum
<i>o</i>	oxidizer
<i>out</i>	outlet
<i>p</i>	propellant
<i>pu</i>	pump
<i>pgs</i>	pressure gas system
<i>t</i>	tank
<i>tot</i>	total
<i>tp</i>	turbopump
<i>tps</i>	turbopump system
<i>tu</i>	turbine
<i>w</i>	water
0	initial conditions in pressure gas tank

1 Introduction

Feed systems for liquid-propellant rocket engines are classically based on either pressurized gas or turbopumps (piston pumps have also been considered for small engines) [1]. An alternative has occasionally been mentioned, based on electric pumps fed by batteries [2, 3, 4], but has not found application, although some conceptual development is currently taking place in the framework of a EU-sponsored project [5]. However, as a result of technological advances over the last decade in the field of electric motors, in particular those based on rare earth permanent magnets (neodymium-iron-boron) [6, 7, 8], and batteries [9, 10, 11, 12], it is now worth re-evaluating the viability of electric-pump feed systems.

In [13] the performance of the proposed system are assessed as compared to the pressure-gas system only, but in the present paper the comparison, in view of the technological advances mentioned above, is extended to turbopump systems as well. It is shown that for some applications the proposed system can already outperform the turbopump one in terms of weight, though not for booster stages. However, it is also shown here to entail several accompanying advantages, which can indeed alter the balance in its favour for some classes of launchers, small-size ones in particular. One of the most stringent requirements in rocket engine design is to keep the inert mass as low as possible, since payload is a quite small fraction of the launcher mass at lift-off. Accordingly, in Sec. 2 the three feed systems mentioned above (i.e., pressure-gas, turbopump, and electric pump) will be compared in terms of their mass. The crucial issue of the identification of appropriate values of figures of merit is discussed in Sec. 3. Numerical examples are then worked out in Sec. 4. A discussion of critical issues of the proposed solution is undertaken in Sec. 5. Conclusions are then drawn in Sec. 6.

2 Evaluation of feed system mass

The mass of the three feed systems under consideration is here estimated; only the main components of each system are considered, whereas minor masses such as plumbing, mounting, valves, pressure regulators and controls are neglected. A similar analysis is given in [13] for the pressure–gas and the electric pump systems, and accordingly it is merely briefly summarized here (though some additional detail concerning the masses of the electric pump system is introduced), whereas a more extended analysis is devoted to the turbopump system.

2.1 Pressure–gas system

The main components of the total mass m_{pgs} of a feed system using pressurized gas are the mass m_g of the pressurizing gas and the masses of the tanks for the gas itself, the fuel and the oxidizer, denoted as $m_{t,g}$, $m_{t,f}$, $m_{t,o}$, respectively:

$$m_{pgs} = m_g + m_{t,g} + m_{t,f} + m_{t,o} \quad (1)$$

A regulated pressure system is considered and, for the sake of conciseness, it is further assumed that the pressure inside the tanks is the same for the two propellants, $p_{t,f} = p_{t,o}$ (this, and similar assumptions in the following, can be easily relieved). The resulting expression [13] for the ratio of the feed system mass to the propellant mass is

$$\frac{m_{pgs}}{m_p} = \left(\frac{C_1}{1 - \kappa_{p1} p_c/p_0} + C_2 \right) p_c = f(p_c, p_0) \quad (2)$$

where the constants are defined as

$$C_1 = \gamma_g \left(\frac{\mathcal{M}_g}{R^0 T_0} + \frac{3}{2} \kappa_{t,g} \frac{\rho_{t,g}}{\sigma_{t,g}} \right) \alpha \kappa_g \kappa_{p1} \kappa_u \quad (3)$$

$$C_2 = \frac{3}{2} \alpha \kappa_{t,p} \kappa_{p1} \kappa_u \frac{\rho_{t,p}}{\sigma_{t,p}} \quad (4)$$

Here p_c is the chamber pressure, p_0 is the initial pressure in the gas tank, T_0 the initial temperature, \mathcal{M}_g is the molar mass of the pressurant, κ_u is a factor accounting for ullage, κ_g is a safety factor for the mass of pressurant, $\kappa_{t,g}$ and $\kappa_{t,p}$ are safety factors for the thickness of the tanks for gas and propellants, respectively; in a similar fashion $\rho_{t,g}$ and $\rho_{t,p}$ are the densities of the wall materials, and $\sigma_{t,g}$ and $\sigma_{t,p}$ the tensile stresses admitted. κ_{p1} is the ratio between propellant tank and chamber pressure

$$\kappa_{p1} = \frac{p_{t,f}}{p_c} = \frac{p_{t,o}}{p_c} \quad (5)$$

and α is defined after

$$\alpha_f = \frac{V_f}{m_p} = \frac{1}{\rho_f} \frac{1}{1 + O/F}, \quad \alpha_o = \frac{V_o}{m_p} = \frac{1}{\rho_o} \frac{O/F}{1 + O/F}, \quad \alpha = \alpha_f + \alpha_o \quad (6)$$

O/F being the oxidizer-to-fuel mass flow ratio, V_f and V_o the fuel and oxidizer volumes, respectively, and $m_p = m_f + m_o$ the total propellant mass.

2.2 Turbopump system

The definition of a turbopump cycle depends on a number of choices. The present example refers to a liquid rocket engine fed with storable propellants NTO (nitrogen tetroxide) as the oxidizer, and MMH (monomethylhydrazine) as the fuel. A gas generator cycle is considered, with a single uncooled turbine with inlet temperature limited to $T_{tu,in}$, typically around 850 – 900 K. However, in systems using MMH, decomposition of fuel (actually, a monopropellant) alone generates temperatures above 1100 K. This requires injection of a third fluid as a coolant (addition of NTO would rise the temperature further), such as water, as in the case of the Viking engines adopted in launchers Ariane 1 through 4 [14]. Then, the main components of the total mass m_{tps} of a turbopump feed system are again a (small) pressurizing gas mass required to avoid cavitation, the masses of the tanks for the gas itself, the fuel,

the oxidizer and the cooling water, plus the mass of the pumps m_{pu} and turbines m_{tu} (actually split between the oxidizer, fuel and water circuits), of the water m_w and propellants (essentially fuel in our case) fed to the gas generator $m_{f,gg}$, and of the gas generator itself m_{gg} . Then

$$m_{tps} = m_g + m_{t,g} + m_{t,f} + m_{t,o} + m_{t,w} + m_{pu} + m_{tu} + m_w + m_{f,gg} + m_{gg} \quad (7)$$

Notice that the propellant mass $m_{f,gg}$ needed for the gas generator is detailed separately for the propellant mass m_p , which is instead meant to be directly usable for propulsion purposes. For water and propellant tanks, in systems using pumps, the tank walls are thin. The thickness as estimated by Laplace's law might be too small to withstand the vehicle acceleration loads. Therefore, a minimum thickness τ_{min} is enforced [13].

The mass of the pumps is related to the mechanical power P_{pu} they deliver, which is proportional to the volume flow rate (propellant plus cooling water volume over burning time) times the pressure rise in the pump. The gas generator is assumed to be fed only with fuel and water, even though things may actually be more complex (some NTO is also usually injected to initiate reaction, otherwise appropriate catalysts must be used), and let W/F denotes the ratio of cooling water and MMH mass flow rates (identified under the requirement of permissible turbine inlet temperature). The total fuel mass (the part usable for propulsion, still denoted as m_f , plus the one fed to the gas generator $m_{f,gg}$) can be put in the form

$$m_{f,tot} = m_f + m_{f,gg} = \beta_f m_f \quad (8)$$

which defines a coefficient $\beta_f > 1$, which will be identified below, see Eq. (18). If the pressure in the gas generator is, for the sake of simplicity, assumed equal to the one in the combustion chamber, then the ratio of pressure rise to chamber pressure can be defined as

$$\kappa_{p3} = \frac{\Delta p_f}{p_c} = \frac{\Delta p_o}{p_c} = \frac{\Delta p_w}{p_c} \quad (9)$$

By further defining

$$\alpha_w = \frac{V_w}{m_p} = \frac{W/F}{\rho_w} \frac{1}{1 + O/F}, \quad \alpha' = \beta_f \alpha_f + \alpha_o + \alpha_w \quad (10)$$

where V_w is the water volume, the required power is

$$P_{pu} = \kappa_{p3} \frac{\alpha' p_c m_p}{t_b} \quad (11)$$

t_b being the burning time. Accordingly, a figure of merit termed pump power density is introduced as the the ratio of the mechanical pumping power to pump mass

$$\delta_{pu} = \frac{P_{pu}}{m_{pu}} \quad (12)$$

The pump mass, for both turbopump and electric pump systems, can then be expressed as

$$m_{pu} = \frac{P_{pu}}{\delta_{pu}} \quad (13)$$

The power required to the turbine driving the pumps also depends on the efficiency η_{pu} of the latter

$$P_{tu} = \frac{P_{pu}}{\eta_{pu}} \quad (14)$$

Accordingly, upon introducing a turbine power density δ_{tu} with definition similar to (12), the turbine mass is evaluated as

$$m_{tu} = \frac{P_{tu}}{\delta_{tu}} \quad (15)$$

The propellant mass $m_{f,gg}$ burned in the gas generator is determined after the power required [15]

$$P_{tu} = \frac{\eta_{tu} \Delta h_{tu,s} m_{f,gg}}{t_b} \quad (16)$$

which in view of Eqs. (14,11) returns $m_{f,gg}$. The quantity $\Delta h_{tu,s}$ is the isentropic equilibrium enthalpy jump when the pressure drops from the value $p_{tu,in}$ at the turbine inlet down to $p_{tu,out}$ at its outlet

$$\Delta h_{tu,s} = [h(p_{tu,in}) - h(p_{tu,out})]_{eq,s} \quad (17)$$

Equations (8, 10, 11, 14, 16) allow identifying the factor β_f as

$$\beta_f = \frac{1 + k (\alpha_o + \alpha_w) p_c}{1 - k \alpha_f p_c} \quad (18)$$

with $k = (1 + O/F) \kappa_{p3} / (\eta_{pu} \eta_{tu} \Delta h_{tu,s})$.

In order to size the gas generator, the stay time (t_s) method is used [16], giving its volume as

$$V_{gg} = \frac{t_s m_{f,gg}}{t_b \rho_{gg}} \quad (19)$$

where ρ_{gg} is the density of gases exhausting from the gas generator. A spherical shape is assumed, so that the wall thickness can be recovered by Laplace's law, and the resulting gas generator mass is

$$m_{gg} = \frac{3 \kappa_{gg} \rho_{m,gg} p_{gg} V_{gg}}{2 \sigma_{gg}} \quad (20)$$

where σ_{gg} is the stress admitted by the gas generator wall material, $\rho_{m,gg}$ its density, p_{gg} the gas generator pressure, and κ_{gg} an appropriate safety factor.

It has to be said that the gas generator exhaust might be used to produce a small contribution to the thrust, but it will be seen in Sec. 4 that this turns out to be basically negligible in the calculations at hand.

A turbopump power density is introduced as

$$\delta_{tp} = 1 / \left(\frac{1}{\delta_{pu}} + \frac{1}{\eta_{pu} \delta_{tu}} \right) \quad (21)$$

and the following quantities are defined

$$D'_1 = \gamma_g \left(\frac{\mathcal{M}_g}{R^0 T_0} + \frac{3}{2} \kappa_{t,g} \frac{\rho_{t,g}}{\sigma_{t,g}} \right) \alpha' \kappa_g \kappa_{p2} \kappa_u \quad (22)$$

$$D'_2 = \frac{3}{2} \alpha_f \beta_f \kappa_{t,p} \kappa_{p2} \kappa_u \frac{\rho_{t,p}}{\sigma_{t,p}} \quad (23)$$

$$D'_3 = (4\pi)^{1/3} (3 \kappa_u \alpha_f \beta_f)^{2/3} \tau_{min} \rho_{t,p} \quad (24)$$

$$D_4 = \frac{3}{2} \alpha_o \kappa_{t,p} \kappa_{p2} \kappa_u \frac{\rho_{t,p}}{\sigma_{t,p}} \quad (25)$$

$$D_5 = (4\pi)^{1/3} (3 \kappa_u \alpha_o)^{2/3} \tau_{min} \rho_{t,p} \quad (26)$$

$$D_9 = \frac{3}{2} \alpha_w \kappa_{t,p} \kappa_{p2} \kappa_u \frac{\rho_{t,p}}{\sigma_{t,p}} \quad (27)$$

$$D_{10} = (4\pi)^{1/3} (3 \kappa_u \alpha_w)^{2/3} \tau_{min} \rho_{t,p} \quad (28)$$

$$D_{11} = \left(1 + \frac{W/F}{1 + O/F} \right) \frac{\alpha' \kappa_{p3}}{\eta_{pu} \eta_{tu} \Delta h_{tu,s}} \quad (29)$$

$$D_{12} = \alpha' \kappa_{p3} \left(\frac{1}{\delta_{tp}} + \frac{3 \kappa_{gg} \rho_{m,gg} p_{gg} t_s}{2 \rho_{gg} \sigma_{gg}} \frac{1}{\eta_{pu} \eta_{tu} \Delta h_{tu,s}} \right) \quad (30)$$

κ_{p2} has a meaning analogous to κ_{p1}

$$\kappa_{p2} = \frac{p_{t,f}}{p_c} = \frac{p_{t,o}}{p_c} \quad (31)$$

the different index is adopted to emphasize the fact that in pump-fed systems the tank pressure is low, thereby $\kappa_{p2} \ll \kappa_{p1}$.

The ratio of the total mass of the turbopump system to the propellant mass can be put, after Eq. (7), in the form

$$\begin{aligned} \frac{m_{tps}}{m_p} = & \frac{D'_1}{1 - \kappa_{p2} p_c/p_0} p_c + \max \left(D'_2 p_c, \frac{D'_3}{m_p^{1/3}} \right) + \max \left(D_4 p_c, \frac{D_5}{m_p^{1/3}} \right) + \max \left(D_9 p_c, \frac{D_{10}}{m_p^{1/3}} \right) + \\ & + D_{11} p_c + D_{12} \frac{p_c}{t_b} = h(p_c, p_0, m_p, t_b) \end{aligned} \quad (32)$$

Notice that while D_4 , D_5 , D_9 and D_{10} are constants (once the values of the different quantities entering in their definition are identified), the quantities D'_1 , D'_2 , D'_3 , D_{11} and D_{12} depends on the chamber pressure through β_f and α' , see Eqs. (18,10). However, it will be shown in Sec. 3 that this dependence is relatively weak.

2.3 Electric pump system

For the total mass m_{eps} of the proposed feed system based on electric pumps, the items being considered are the (still small) pressurizing gas mass, the masses of the tanks for the gas itself, the fuel and the oxidizer, plus the masses m_{pu} of the pumps, m_{em} of the electric motor(s), m_{inv} of the inverter (the power electronic device driving the electric motor), and m_b of batteries

$$m_{eps} = m_g + m_{t,g} + m_{t,f} + m_{t,o} + m_{pu} + m_{em} + m_{inv} + m_b \quad (33)$$

For the first five terms at the right-hand-side, the expressions given in Sec. 2.2 apply, in particular the pump mass can be expressed after (13) as

$$m_{pu} = \frac{P_{pu}}{\delta_{pu}} = \frac{\kappa_{p3} \alpha p_c m_p}{\delta_{pu} t_b} \quad (34)$$

The electric motor(s) mass is recovered similarly to Eq. (15), after defining a power density thereof as a ratio between mechanical output power and motor mass

$$\delta_{em} = \frac{P_{em,out}}{m_{em}} \quad (35)$$

which accordingly gives

$$m_{em} = \frac{P_{pu}/\eta_{pu}}{\delta_{em}} = \frac{\kappa_{p3} \alpha}{\eta_{pu}} \frac{p_c m_p}{\delta_{em} t_b} \quad (36)$$

In a similar fashion, after introducing the efficiencies of the electric motor η_{em} and of the inverter η_{inv} , and a power density of the latter

$$\delta_{inv} = \frac{P_{inv,out}}{m_{inv}} \quad (37)$$

the inverter mass can be estimated as

$$m_{inv} = \frac{P_{pu}/\eta_{pu}}{\eta_{em} \delta_{inv}} = \frac{\kappa_{p3} \alpha}{\eta_{pu} \eta_{em}} \frac{p_c m_p}{\delta_{inv} t_b} \quad (38)$$

The batteries are limited in both energy and power capacity; therefore, their mass is dictated by the most stringent of the two constraints. After defining a global efficiency of the electric pump system as

$$\eta_{ep} = \eta_{pu} \eta_{em} \eta_{inv} \quad (39)$$

the electric energy required to drive the pumps over the whole engine operating time t_b is

$$E_e = \frac{P_{pu} t_b}{\eta_{ep}} = \frac{\alpha \kappa_{p3}}{\eta_{ep}} m_p p_c \quad (40)$$

and the corresponding power required is

$$P_e = \frac{E_e}{t_b} \quad (41)$$

Upon introducing the power density δ_P (electric power per unit mass) and the energy density δ_E (electric energy per unit mass) of the batteries, their mass m_b is accordingly determined as

$$m_b = \kappa_b \max \left(\frac{P_e}{\delta_P}, \frac{E_e}{\delta_E} \right) \quad (42)$$

where a factor κ_b is introduced to account for design margins. The following additional constants are also introduced

$$D_1 = \gamma_g \left(\frac{\mathcal{M}_g}{R^0 T_0} + \frac{3}{2} \kappa_{t,g} \frac{\rho_{t,g}}{\sigma_{t,g}} \right) \alpha \kappa_g \kappa_{p2} \kappa_u \quad (43)$$

$$D_2 = \frac{3}{2} \alpha_f \kappa_{t,p} \kappa_{p2} \kappa_u \frac{\rho_{t,p}}{\sigma_{t,p}} \quad (44)$$

$$D_3 = (4\pi)^{1/3} (3\kappa_u \alpha_f)^{2/3} \tau_{min} \rho_{t,p} \quad (45)$$

$$D_6 = \alpha \kappa_{p3} \left(\frac{1}{\delta_{pu}} + \frac{1}{\eta_{pu} \delta_{em}} + \frac{1}{\eta_{pu} \eta_{em} \delta_{inv}} \right) = \alpha \kappa_{p3} \mu_{ep} \quad (46)$$

$$D_7 = \frac{\alpha \kappa_b \kappa_{p3}}{\eta_{ep} \delta_P} \quad (47)$$

$$D_8 = \frac{\alpha \kappa_b \kappa_{p3}}{\eta_{ep} \delta_E} \quad (48)$$

Notice that in (46) a more concise expression in terms of the global electric pump specific mass μ_{ep} is also given. After Eq. (33), the ratio of the total electric pump system mass to the propellant mass can be put in the form

$$\frac{m_{eps}}{m_p} = \frac{D_1}{1 - \kappa_{p2} p_c / p_0} p_c + \max \left(D_2 p_c, \frac{D_3}{m_p^{1/3}} \right) + \max \left(D_4 p_c, \frac{D_5}{m_p^{1/3}} \right) +$$

$$+ D_6 \frac{p_c}{t_b} + \max \left(\frac{D_7 p_c}{t_b}, D_8 p_c \right) = g(p_c, p_0, m_p, t_b) \quad (49)$$

3 Estimation of figures of merit

In the following, attention is devoted to a liquid-propellant rocket engine burning storable propellants. Indeed, as the inspiring approach of the electric pump system is simplicity, it appears justified to focus the analysis on systems relatively simple *per se*, thereby ruling out cryogenic propellants (though actually liquid oxygen and liquid methane might also be included). In particular, monomethyl hydrazine (MMH) and nitrogen tetroxide (NTO) are considered as fuel and oxidizer, respectively, and helium as the pressurizing gas.

In order to define the masses of the different feed system options envisaged, care must be taken in evaluating the different parameters and figures of merit involved. These are subscripted as follows: 1) pressure-gas system, 2) turbopump system, and 3) electric-pump system. As far as the pumps are concerned, a somewhat different criterium could in principle be adopted for systems 2) and 3), see below. For the turbopump system, reference is made to the Titan II first-stage one, working on storable propellants. The turbine efficiency is accordingly assumed 56%, while the pump efficiency is taken as 68%; as far as power density is concerned, a value 18 kW/kg is assumed with reference to axis power.

For the electric pump system, a somewhat higher pump efficiency could be assumed, at the expense of a lower pump power density, by adopting a bladed diffuser at the pump discharge. This would significantly reduce the battery mass, see Eqs. (39–42), which in many cases takes the largest share of the feed system mass. However, this would require a design analysis and optimization of the whole assembly pump–electric motor–batteries, which is beyond the scope of the present work. Accordingly, a 68% efficiency is still assumed for the pumps. For the pump power density, a value of 22 kW/kg is extrapolated from the Titan turbopump data.

In order to provide a fair comparison of the proposed system 3 with respect to 2, values are chosen so as to ensure a highly effective turbine operation. Accordingly, while ruling out blade cooling and exotic alloys, a relatively high turbine inlet temperature $T_{tu,in}$ is assumed, see Tab. 1. Pressure drops in the plumbing are neglected. Open-cycle operation is assumed, and a quite high value for the turbine pressure ratio is adopted. The gas generator is assumed to operate at the same pressure as the main chamber; an optimistic stay time is chosen in order to ensure a lightweight design [17]. Brushless DC electric motors are considered for system 3. The motor power density and efficiency adopted here, as determined from datasheets¹, are conservative, to avoid producing results biased in favor of the proposed system. It is as well to remark that motors featuring an even higher power density are available², but when the presumable mass of the cooling system is taken into account (see Sec. 5) a value of δ_P about the same (actually, somewhat higher) as the one adopted here is recovered. The inverter properties are taken after data by Castle Creations³. As far as batteries are concerned, different manufacturing technologies are available. The need for a high power density is apparent, but the energy density too becomes a limiting factor for long operating times. Therefore, a technology offering both high power and energy densities is sought. Among the most promising technologies there are Lithium-Polymer (Li-Po), Lithium-Ion (Li-Ion), and Lithium-Sulfur (Li-S) cells. The values of merit figures assumed for the different batteries are based on data reported in [18, 21] and in datasheets by Thunder Power and Sion Power⁴. Criteria for selecting the batteries are indicated in Sec. 4. Finally, both the den-

¹Plettenberg Electromotoren, Predator 37 and Predator 30 datasheets, website www.plettenberg-motoren.com; Maxx Products International Inc., Himax HC5030-390 datasheet, website www.maxxprod.com.

²YASA Motors, Model YASA 400, data-sheet, 2012, website www.yasamotors.com.

³Castle Creations Inc., Phoenix ICE HV ESC datasheets, website www.castlecreations.com.

⁴Thunder Power Li-Po Battery Data Sheet, 2250mAh, 5-Cell/5S (18.5V 30C/60C), website www.thunderpowerrrc.com; Sion Power, Lithium Sulfur Rechargeable Battery Data Sheet, www.sionpower.com.

sity and the maximum tensile strength of the materials adopted to manufacture all tanks, and the gas generator, must be identified. Kevlar is elected for the gas tank, while aluminum alloy is chosen for the propellant tanks; for the GG, Hastelloy C is selected. Table 1 recaps the values of the different quantities, adopted in the subsequent comparison in Sec. 4.

p_0	20 MPa,	p_c	3 MPa
δ_{em}	3.8 kW/kg,	δ_{pu}	22 kW/kg
δ_{inv}	60 kW/kg,	δ_{tp}	18 kW/kg
η_{em}	0.8,	η_{inv}	0.85
η_{pu}	0.68,	η_{tu}	0.56
$T_{tu,in}$	900 K,	t_s	10 ms
$p_{tu,in}/p_{tu,out}$	20,	$\Delta h_{tu,s}$	1060 kJ/kg
W/F	0.328,	ρ_{gg}	6.3 kg/m ³
$\delta_{P,Li-Po}$	6000 W/kg,	$\delta_{E,Li-Po}$	130 Wh/kg
$\delta_{P,Li-Ion}$	2000 W/kg,	$\delta_{E,Li-Ion}$	220 Wh/kg
$\delta_{P,Li-S}$	1200 W/kg,	$\delta_{E,Li-S}$	350 Wh/kg
$\rho_{t,g}$	1700 kg/m ³ ,	$\sigma_{t,g}$	3300 MPa
$\rho_{t,p}$	2800 kg/m ³ ,	$\sigma_{t,p}$	455 MPa
$\rho_{m,gg}$	8890 kg/m ³ ,	σ_{gg}	524 MPa (at 1033 K)

Tab. 1: Values of parameters and figures of merit.

Notice that the ideal isentropic enthalpy jump in the turbine $\Delta h_{tu,s}$ is computed by enforcing the indicated inlet and outlet turbine conditions, which implies diluting the MMH fuel decomposition products with water in a mass ratio W/F as indicated. Further, the value of η_{ep} is determined after Eq. (39) as about 0.462, and that of the specific electric pump mass after Eq. (46) as 0.463 kg/kW. The last quantity in particular exhibits an abundant order-of-magnitude improvement with respect to early assumptions in [13], though it is also observed that the overall efficiency is somewhat reduced. Notice that the dominant term in μ_{ep} is the electric motor mass.

Values in Tab. 1 are supplemented by various additional indices, already identified in [13], as reported in Tab. 2. Notice in particular that for the safety factor relating to tank wall thickness, different values are assumed for metallic and composite tanks; further, the former refers to the yield strength, the latter to the ultimate strength. A safety factor 1.2 is adopted for the battery mass, in order to allow the batteries to operate somewhat under-rated to prevent overheating and possible failure, and also to make room for a significant redundancy in the case of partial failure.

κ_{p1}	=	1.8	κ_{p2}	=	0.3	κ_{p3}	=	1.5
κ_g	=	1.3	$\kappa_{t,g}$	=	2.4	$\kappa_{t,p}$	=	1.25
κ_u	=	1.05	κ_b	=	1.2	τ_{min}	=	1 mm
γ_g	=	1.667	\mathcal{M}_g	=	4.0026 kg/kmol	T_0	=	288.15 K
ρ_o	=	1431 kg/m ³	ρ_f	=	874 kg/m ³	ρ_w	=	997 kg/m ³
O/F	=	ρ_o/ρ_f						

Tab. 2: Values of ancillary quantities.

Figure 1 gives the resulting trend, for this set of values, of the quantities α' and β_f , as a function of chamber pressure, emphasizing a relatively weak dependance. It is seen that β_f grows about linearly with chamber pressure, with the amount of extra fuel needed for the gas generator reaching at most 10% of the usable fuel mass m_f for high chamber pressure (10 MPa).

4 Results

The three feed system concepts indicated in Sec. 1 are now tentatively compared in terms of their own mass, for an application involving a relatively small-size stage (propellant mass in the range 1000 to 20000 kg).

Expressions (2,32,49) point out to the fact that the key structural mass index under consideration, i.e., the ratio m_{pfs}/m_p of feed system mass to usable propellant mass,

is a function of chamber pressure, initial pressurant pressure and, for pump-based systems, of the burning time and eventually of the propellant mass itself when the tank thickness attains the minimum allowed value τ_{min} . The dependence of the above ratio on the design quantities indicated is therefore investigated for the three feed options, by identifying a set of reference values, and then varying design parameters one at a time. The reference values are identified as $p_c = 3$ MPa, $p_0 = 20$ MPa, $m_p = 3000$ kg; for the burning time two reference values are considered, $t_b = 120$ and 1000 s, the former representative of a typical booster, the second of a last stage for injection into orbit. Incidentally, for the turbopump system, the ratio of the thrust which can be obtained by the gas generator exhaust to the thrust developed by the main nozzle turns out, under the present assumptions, to be less than 0.4%.

It must be emphasized that the choice of the most appropriate kind of cells, for the electric pump system, is heavily dependant on the value of the burning time t_b . For short burning times the limiting factor is the battery power density, whereas for longer times the limit is on the energy density. Li-Ion and Li-S cells offer a higher energy density with respect to Li-Po ones; however, they feature a reduced power density. The reduction in power density is of interest only for applications involving short burning times, i.e., lower stages. The effect on the ratio of feed system mass over propellant mass of a stage powered by an engine operating in the reference conditions mentioned above, with varying burning time, is shown in Fig. 2 (incidentally, the axis ranges are chosen so as to evidentiate the effect of interest). It is seen that each single kind of cells is most suited for operation within a well-defined range of t_b values. For relatively short burning times, Li-Po batteries result in the lightest feed system, while in the range between 234 and 660 s Li-Ion batteries are the most convenient ones; lastly, Li-S batteries are the most appropriate choice for burning times over 660 s. Incidentally, notice that battery manufacturers indicate a minimum discharge time. In principle, the optimal burning time from the standpoint of battery profit is given by

$$t_{b,opt} = \delta_E/\delta_P \quad (50)$$

At this limiting value, the battery is fully exploited, working at both maximum power density and maximum energy density. Indeed, the curves relative to the different cell types exhibit a knee for a burning time such that the battery operates at condition (50), i.e., 78 s for Li–Po cells, 396 s for Li–Ion, and 1050 s for Li–S ones. Then, the battery mass is power–constrained up to a burning time $t_{b,opt}$, and energy–constrained thereafter. However, the mass of the other feed system components, electric pumps in particular (see also Fig. 3 below), most generally leads to adopting a value of t_b different from the one given by (50).

In order to clarify this issue, a breakdown of the electric pump feed system mass is shown in Fig. 3, detailing the percentage of the mass due to the pressurant, the tanks (fuel, oxidizer, and pressurant), the assembly of the electric motor, the pump and the inverter, and the batteries. It is seen that the mass of the battery pack takes a major share of the whole system mass, and is directly related to the power (for operating times shorter than $t_{b,opt}$) or the energy required by the electric motors throughout their operating life (for longer times). The three peaks in the Figure (upper curve, corresponding to local minima for battery mass) indicate the transition between the two conditions (power/energy constraint) for (left to right) Li–Po, Li–Ion, Li–S batteries, respectively.

Figure 4 shows the trend of the feed system mass over propellant mass as a function of the burning time t_b , for the three feed system options in Sec. 2. It is seen that while this ratio remain constant for the pressure–fed system, it decreases instead with burning time for the two pump–based systems, though reaching a near–asymptote quite early, especially the turbopump one. Systems using pumps exhibit a clear advantage over the pressure–gas one, owing to their much lighter tanks. The proposed electric pump system turns out to be somewhat heavier with respect to the turbopump one for short values of the burning time, less than 459 s, but lighter

thereafter. In particular, for a typical booster burning time, e.g., 120 s, the penalty is limited to about 1.8% of the propellant mass, whereas for a value more typical of a last stage, e.g., 1000 s, a significant bonus of 0.6% is obtained by using the proposed system. Bumps in the curve for the electric pump system (at $t_b = 234$ and 660 s) correspond to switching to a different battery type. Notice that for pump-based systems the thickness of the propellant tank walls attains the specified minimum value τ_{min} , under the assumed data, when the propellant mass is less than 4870 kg. This minimum thickness also holds for the cooling water tank in turbopump systems, due to its much smaller size.

Figure 5 shows the trend of the feed system mass over propellant mass as a function of the propellant mass, for the two values of the burning time under consideration. The above ratio again turns out to be constant for the pressure-gas system, and to initially decrease for the pump-based systems. In particular, for the electric pump system the ratio attains a constant value for a propellant mass larger than the above-mentioned limit of 4870 kg, since in Eq. (49) the terms in D_2 and D_4 overwhelm the alternative ones in D_3 and D_5 , respectively. The turbopump system shows instead a very slightly diminishing trend even beyond $m_p = 4870$ kg, due to the fact that in any case the thickness of the water tank walls is dictated by τ_{min} ; accordingly in Eq. (32) the term in D_{10} is still larger than the one in D_9 , and a dependance on m_p remains, though quite weak (due to the small cooling water mass required). While the turbopump system results to be the lightest one for $t_b = 120$ s, it is especially remarkable that for $t_b = 1000$ s the electric pump system results to be significantly lighter than the alternatives. This confirms that the electric pump system is most suitable for long burning times. It is also seen that, for each value of t_b , the gap between the two pump-based systems remains quite constant with m_p .

In a similar fashion, Fig. 6 shows the trend of the feed system mass over propellant mass as a function of the combustion chamber pressure, for the two values of the burning time. A marked increasing trend is observed for all feed system, which in particular makes the pressure-fed system unsuited for high chamber pressures. A

milder trend is observed for pump-based systems. For a burning time of 120 s, the electric pump system features a penalty over the turbopump one growing from 1.2% to 6.2% as p_c spans the range from 2 to 10 MPa. Again, for $t_b = 1000$ s the electric pump system is the lightest one, featuring in particular a bonus over the turbopump one from 0.5% to 2% in the same range.

Lastly, Fig. 7 indicates the effect of the initial helium pressure p_0 . A marked decreasing trend is observed for the pressure-gas system, albeit with a trend toward saturation for very high values of p_0 . Pump-based systems both instead exhibit a barely perceivable decreasing trend.

Notice that the curves referring to the electric pump system all exhibit a marked improvement with respect to the ones reported in the original work [13], thanks to the new electric motors and the improved batteries.

Attention is now focused on the most significant quantity for the evaluation of a launcher performance, i.e., the overall payload ratio λ between the payload mass and the launcher mass at lift-off. In order to determine this quantity, some working assumptions are introduced: the launcher is assumed to be three-stage, all fed by NTO/MMH, the (average) effective exhaust velocity for the first stage is assumed to be 2700 m/s, whereas it is set at 2900 m/s for the upper stages; a 3% reserve propellant is assumed, and the structural mass of each stage (including interstages) is assigned as the feed system mass plus 4% of the propellant mass. The effective Δv for injection into LEO is assumed as 9300 m/s, which is further hypothesized to be evenly partitioned among the individual stages. A burning time of 120 s is taken for the first and second stage, whereas for the third a value of 1000 s is assumed. Such assumptions, although partly objectionable, allow a first assessment of the performance of a launcher under the three different feed options under consideration. Figure 8 reports the resulting overall payload ratio as a function of the total propellant loading (i.e., the sum of the propellant mass of the three stages). The Figure confirms that pump-systems offer better performance with respect to pressure-gas

ones, the latter giving a payload ratio constant at about 0.96%. Pump-based systems give a payload ratio slightly increasing with total propellant mass, and in particular (the key point in this assessment), the turbopump system appears to offer some advantage over the proposed electric pump system, which is however seen to span the limited range 6 to 9% on a relative basis, with an increasing trend with respect to total propellant loading. This means that a wholly electric pump rocket will be economically competitive with a turbopump-fed rocket if the former solution allows for a launch cost reduction of approximately the same (small) order. At any rate, adopting a turbopump system for the first two stages and an electric pump system for the third one would give the highest λ among all configurations.

5 Discussion

From results shown above it is seen that in general the electric pump system gives structural masses much lower than the pressure-gas system (especially for high-pressure combustion chambers), still appreciably higher than turbopump systems for short burning times, but already significantly lower for long burning times. This indicates a double field of application of the proposed system. First, it can advantageously replace classical feed systems at a reasonable cost in upper stages (currently either turbopump or pressure-fed) and spacecrafts (always pressure-fed), with an accompanying reduction of inert mass, particularly remarkable with respect to pressurized systems. Secondly, it can find an application also for lower stages in small launchers, for which the high development cost of a turbopump system is not justified, whereas the electric pump one can still be affordable, in particular due to the absence of hot sections. Incidentally, a turbopump involves very high temperature gradients along the shaft, with ensuing mechanical problems, and a problematic handling of propellant flow through the pumps. Piston pumps have also been proposed for small stages [19]; however, they still imply hot parts, and their design is less easily scaleable. A test rig based on an electric pump system, though based on

off-the-shelf components, is under investigation at Sapienza Università di Roma as a proof-of-concept [20].

Quite obviously, results are sensitive to the values assumed for the figures of merit. Accordingly, relative sensitivities of the overall payload ratio to such figures are introduced as

$$s_{\delta_{inv}} = \delta_{inv} \frac{\partial \lambda}{\partial \delta_{inv}}, \quad s_{\delta_{em}} = \delta_{em} \frac{\partial \lambda}{\partial \delta_{em}}, \quad s_{\delta_{pu}} = \delta_{pu} \frac{\partial \lambda}{\partial \delta_{pu}}, \quad s_{\delta_P} = \delta_P \frac{\partial \lambda}{\partial \delta_P} \quad (51)$$

for the power densities of the inverter, electric motor, pumps and batteries, respectively, then

$$s_{\delta_E} = \delta_E \frac{\partial \lambda}{\partial \delta_E} \quad (52)$$

for the energy density of the batteries, and as

$$s_{\eta_{inv}} = \eta_{inv} \frac{\partial \lambda}{\partial \eta_{inv}}, \quad s_{\eta_{em}} = \eta_{em} \frac{\partial \lambda}{\partial \eta_{em}}, \quad s_{\eta_{pu}} = \eta_{pu} \frac{\partial \lambda}{\partial \eta_{pu}} \quad (53)$$

for the efficiencies of the inverter, electric motor and pumps, respectively. Such definitions result in dimensionless quantities, thereby allowing to compare the sensitivity to different figures of merit on a common ground. Resulting values for the case considered in Sec. 4 depend very weakly on the propellant mass, thereby they are shown here only for a single, intermediate value thereof, taken as 10000 kg. Figure 9 show sensitivities for the case at hand. It is seen that among the electric pump components, the controlling factor in terms of power density is the electric motor. This is because its assumed value (3.8 kW/kg) is far lower than those for the inverter (60 kW/kg) and the pumps (22 kW/kg), i.e., it is the heaviest component. The sensitivity to the battery power density turns out to be rather small since the batteries of the first two stages operate energy-constrained ($t_b = 120$ s, greater than the ‘optimal’ value of 78 s for Li-Po cells), while the third stage operates power-constrained, but very close to condition (50) ($t_b = 1000$ s, against an ‘optimal’ value

of 1050 for Li-S cells). Moving on the same grounds, it can be easily inferred that the sensitivity to the battery energy density is quite high, as confirmed by Fig. 9, indicating it to be nearly six times that to the battery power density.

As far as the effect of the efficiencies of the electric pump components is concerned, the largest improvement can be obtained by raising the pump one, since it is taken as low as 0.68; smaller effects are anticipated for the electric motor efficiency (taken as 0.8) and the inverter one (taken as 0.85).

This sensitivity analysis accordingly indicates what are the components which, if improved, would allow to attain a payload ratio close to that of a turbopump-fed rocket. The most influent components are the pumps, as the payload ratio could be greatly increased by improving their efficiency. Although this problem is somewhat outside the focus of the present paper, a significant improvement can be obtained by using a bladed diffuser, though at the expense of weight, as already observed. The electric motor has a strong impact, both in terms of efficiency and power density; notice that an improvement of the efficiency would also entail a higher power density, owing to the ensuing reduced cooling requirements. The efficiency of the inverter is also important (improved efficiencies in general reduce the electric power/energy density requirements, then reducing the battery mass). As far as batteries are concerned, the prime requisite is a high energy density, as already observed.

It must be considered that both motor and cell technologies are evolving very rapidly, resulting in ever increasing efficiency and power density (for the former), and power and energy densities (for the latter). As far as motors are concerned, Halbach units claiming peak power density up to 8.7 kW/kg and efficiency 0.97 appear to be available, see footnote 2, though such figures may need to be downrated somewhat for rocket operation due to extra cooling requirements and harsh operating conditions. In particular, values of 6 kW/kg and 0.92 are used below. As far as batteries are concerned, Li-Ion and Li-S cells with an energy density approaching 400 Wh/kg are now in the final stage of development, see [18] and data by Envia Systems⁵.

⁵“Envia Systems hits 400 Wh/kg target with Li-ion cells; could lower Li-ion cost to \$180/kW”,

When such hypothetical advanced components are adopted to power the electric pump system, they result in an overall payload ratio very close to that granted by a turbopump-fed rocket (incidentally, it can be noted that the improvement in the energy density for the last stage batteries is inessential, since the feed system is power-constrained). For a propellant mass of 10000 kg, Fig. 8 indicates a value of 0.0176 for the turbopump system and 0.0162 for the electric pump one; the latter value increases to 0.0170 when adopting such advanced components. Future improvements, which are quite likely, could further close the gap.

Despite its supposed advantages, the electric-pump fed system features its own critical points. The electric motor and the inverter, and possibly also the battery pack, need to be cooled during operation, as power conversion inefficiencies result in heat release. For short burning times, heat-sink cooling may suffice. In this context, it is as well to remark that using many smaller electric motors, rather than a single one, favours both refrigeration (thanks to the larger ratio of surface area to volume) and lightweight design (as smaller motors can rotate at higher speeds, thereby attaining higher power density), though implying somewhat more complex plumbing. It also increases the reliability of the system, as failure of a single motor would still allow operation to continue, albeit at a somewhat reduced propellant flowrate, then thrust, roughly compensated by an ensuing longer burning time. The launch will need to be aborted only if failure takes place in the first few seconds after lift-off, when the launcher thrust-to-weight ratio is still only slightly above unity, and even a limited reduction of thrust can accordingly be fatal. As far as batteries are concerned, in applications to spacecrafts, attention should also be devoted to protect them from sub-freezing temperatures, by means of an appropriate thermal control system. Problems related to electromagnetic compatibility are presumably similar to conventional DC brushed motors [22].

Still with reference to Fig. 3, it is as well to remark that, whereas in turbopump systems achieving a high turbomachinery efficiency is most generally not an issue,

website www.greencarcongress.com/2012/02/envia-20120227.html.

owing to the very limited fraction of the propellant energy consumed by the feed system, and weight is instead the main focus, the situation is different for the electric pump system. The battery mass is inversely proportional to the efficiencies of the different components, the pumps in particular, since they are usually the least efficient component. The proposed system could therefore take great advantage by the adoption of more efficient pumps, featuring a bladed diffuser, which would anyway imply a higher mass. However, from Fig. 3 it is seen that the pump mass is a negligible percentage of the electric pump system mass for long burning times. A detailed balance of the system requires anyway a coupled optimization of the design of the pumps, the electric motors, and the inverter. As compared to Fig. 9 of Ref. [13], Fig. 3 emphasizes a markedly reduced weight of the pump–motor–inverter group, thanks to the use of the above–mentioned advanced components.

The electric pump systems exhibits some specific features which the designer can take advantage of in the engine design process. The possibility of controlling the engine operation *via* the power input to the electric motor offers in principle some important potentialities. Should the liquid propellant engine experience combustion instabilities, an appropriately tailored input signal could be used to cancel them. Actually, the instability frequency range which can be dealt with by such an approach cannot be assessed *a priori*, since it requires a careful analysis of the response of the electric motor and the pumps. In general, using smaller motors as suggested above involves a faster response, and therefore possible control of higher frequency instability. Further, in the light of developing low–cost systems for small launchers, the proposed system offers the chance of adopting ablative coatings to protect the thrust chamber walls, without risking an early detachment of the thermal protection, thanks to the possibility of enforcing a ‘soft’ start by appropriately tailoring the electric input sequence. When throttleability is a key demand, such as in propulsion systems for soft landing, the proposed approach offers a definite advantage, albeit the limit in this case is most often rather dictated by the injectors performance under conditions of widely varying mass flow rates.

6 Conclusions

Results in Sec. 4, based on the use of advanced electric motors and batteries, imply a remarkable extension of the possible field of application of the feed system based on electric pumps, with respect to the original estimate in [13]. In addition to the already established possible application to systems involving a relatively long burning time and a relatively high chamber pressure, exhibiting definite advantages over pressure–gas systems in term of feed system mass and effective exhaust velocity, present results suggest applicability to the upper stage of a launcher, and possibly lower stages too. Although for short burning times turbopump systems are still somewhat lighter, the electric pump system may well result to be cheaper, due to the absence of high temperature components, and in addition offers an easier controllability.

The proposed system features great potential for improvement, e.g., by adopting more efficient pumps (though at the expense of pump mass) the battery mass, which is one of the most important component of the feed system mass, could be greatly reduced. The same holds for the efficiencies of the other components, electric motors in particular. Further, advanced cells currently under development could make the proposed system lighter than the turbopump one, even for applications involving short burning times, i.e., booster stages.

References

- [1] Sutton, G.P. and Biblarz, O., *Rocket Propulsion Elements*, 7th Ed., Wiley, New York, 2001, pp. 203–226.
- [2] Chazen, M.L., “Pump-fed Satellite Delivery Stage Engine Technology”, SAE paper 841528, 1984.
- [3] Johnsson, G. and Bigert, M., “Development of Small Centrifugal Pumps for an Electric Propellant Pump System”, *Acta Astronautica*, vol. 21, No. 6/7, pp. 429–438, 1990.
- [4] Schneider, S.J., Veres, J.P., Hah, C., Nerone, A.L., Cunningham, C.C., Kraft, T.G., Tavernelli, P.F. and Fraser, B., “Satellite Propellant Pump Research”, paper AIAA–2005–3560, 2005.
- [5] Lemaitre, A. and Marciquet, C., “Propellant Electric Pump for Low Thrust Cryogenic Propulsive Systems”, 4th EUCASS, St. Petersburg, July 2011.
- [6] Hanselman, D.C., *Brushless Permanent Magnet Motor Design*, 2nd Ed., Magna Physics Pub., Hillsboro, 2006.
- [7] Gieras, J.F., *Advancements in Electric Machines*, Chaps. 3 and 10, Sect. 10.3.3, Springer, Berlin, 2008.
- [8] Gieras, J.F., Wang, R.–J. and Kamper, M.J., *Axial Flux Permanent Magnet Brushless Machines*, 2nd Ed., Springer, Berlin, 2008.
- [9] Munshi, M.Z.A. (Ed.), *Handbook of Solid State Batteries and Capacitors*, Chaps. 18, 19 and 21, World Scientific Publ., Singapore, 1995.
- [10] Linden, D., *Handbook of Batteries*, 3rd. ed., Part 5: Advanced Batteries for Electric Vehicles and Emerging Applications, McGraw–Hill, New York, 2001.

- [11] van Schalkwijk, W. A. and Scrosati, B. (Eds.), *Advances in Lithium–Ion Batteries*, Kluwer, New York, 2002.
- [12] Nazri, G.–A. and Pistoia, G. (Eds.), *Lithium Batteries. Science and Technology*, Springer, New York, 2009.
- [13] Soldà, N. and Lentini, D., “Opportunities for a Liquid Rocket Feed System Based on Electric Pumps”, *J. Prop. P.*, Vol. 24, No. 6, 2008, pp. 1340–1346.
- [14] Kiselev, A.I., Medvedev, A. and Men’shikov, V.A., *Astronautics: Summary and Prospects*, Springer, Wien, 2003, pp. 65–67.
- [15] Humble, R.W., Lewis, D. and Sackheim, R., “Liquid rocket propulsion systems”, in *Space Propulsion Analysis and Design* (Humble, R.W., Henry, G.N. and Larson, W.J., Eds.), McGraw–Hill, New York, 1995.
- [16] NASA, Turbopump Systems for Liquid Rocket Engines, NASA SP–8107, August 1974.
- [17] NASA, Liquid Propellants Gas Generators, NASA SP-8081, March 1972.
- [18] Mikhaylik, Yu., Kovalev, I., Xu, J. and Schock, R., “Rechargeable Li–S battery with Specific Energy 350 Wh/kg and Specific Power 3000 W/kg, 213th ECS Meeting, The Electrochemical Society, Abstract #112, 2008.
- [19] Warwick, G., “XCOR Demonstrates Piston Pump Rocket Engine”, *Aviation Week & Space Technology*, June 9, 2010.
- [20] Spiller, D., Stabile A. and Lentini, D., “Experimental Study of an Electric Pump Feed System for Liquid Propellant Rocket Engines”, submitted, 2012.
- [21] Gitzendanner, R., Puglia, F. and Santee, S., “Advances in the Energy and Power Density of Lithium–Ion Batteries for Undersea Applications”, UDT 2009, Cannes, 2009.

- [22] Gieras, J.F. and Wing, M., *Permanent Magnet Motor Technology*, Chap. 12, Sect. 12.8, Dekker, New York, 2002.

List of Figures

1. Quantities α' and β_f as a function of chamber pressure.
2. Feed system to propellant mass ratio as a function of engine burning time, for the electric pump system fed by different batteries.
3. Breakdown of the electric pump feed system mass as a function of engine burning time.
4. Feed system to propellant mass ratio as a function of engine burning time. Solid line, pressure-gas; dash-dotted line, turbopump; dashed line, electric pump system.
5. Feed system to propellant mass ratio as a function of propellant mass, for two values of the burning times t_b . Solid line, pressure-gas; dash-dotted line, turbopump; dashed line, electric pump system.
6. Feed system to propellant mass ratio as a function of chamber pressure, for two values of the burning times t_b . Solid line, pressure-gas; dash-dotted line, turbopump; dashed line, electric pump system.
7. Feed system to propellant mass ratio as a function of initial gas pressure, for two values of the burning times t_b . Solid line, pressure-gas; dash-dotted line, turbopump; dashed line, electric pump system.
8. Overall payload ratio for an orbital launcher, for the different feed system options. Solid line, pressure-gas; dash-dotted line, turbopump; dashed line, electric pump system.
9. Sensitivity of the overall payload ratio to the different figures of merit.

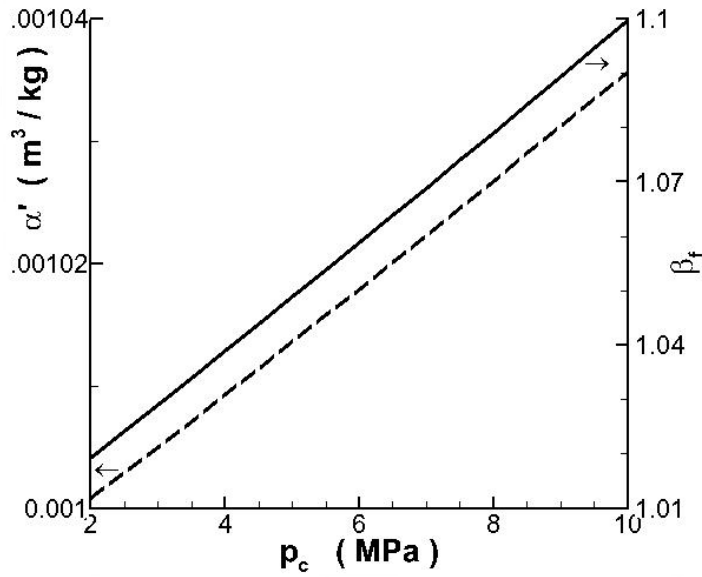


Figure 1:

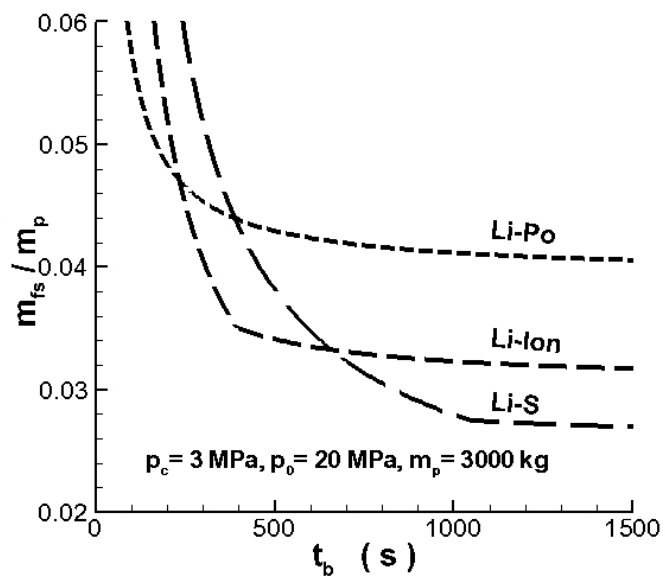


Figure 2:

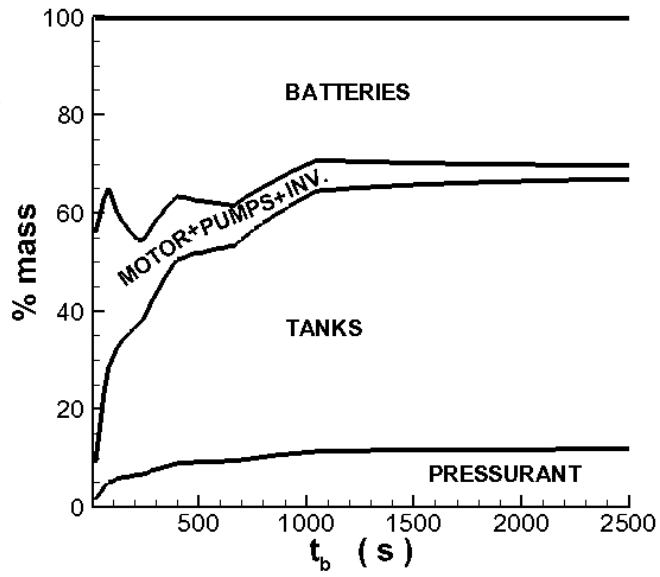


Figure 3:

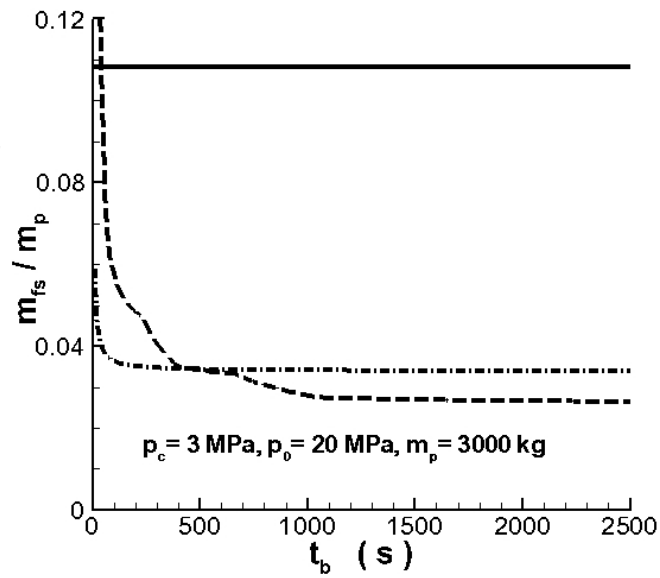


Figure 4:

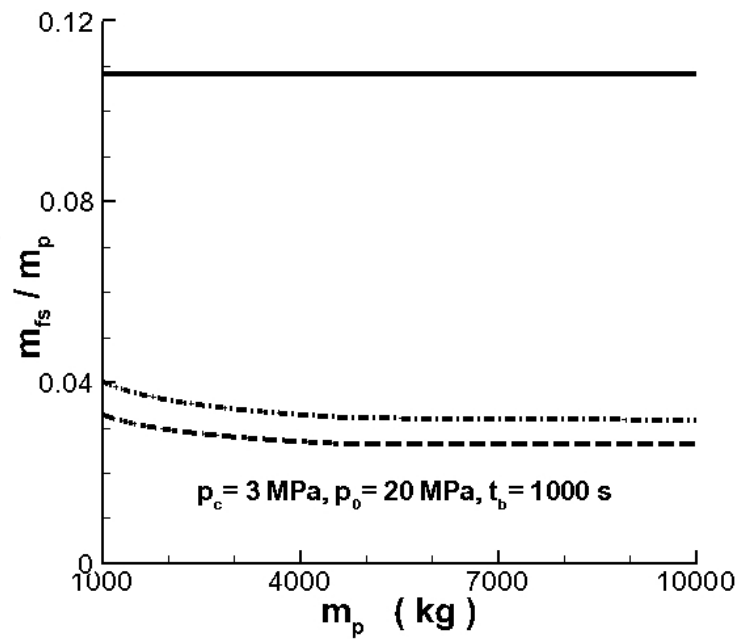
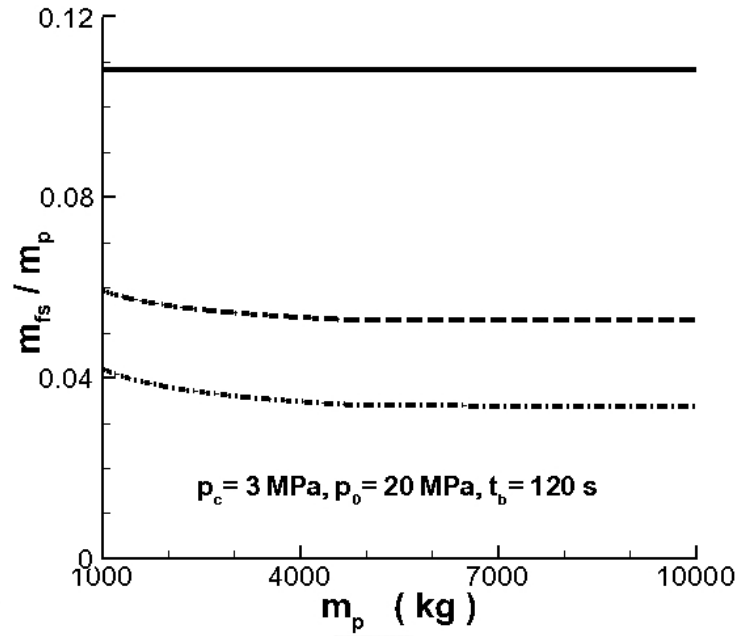


Figure 5:

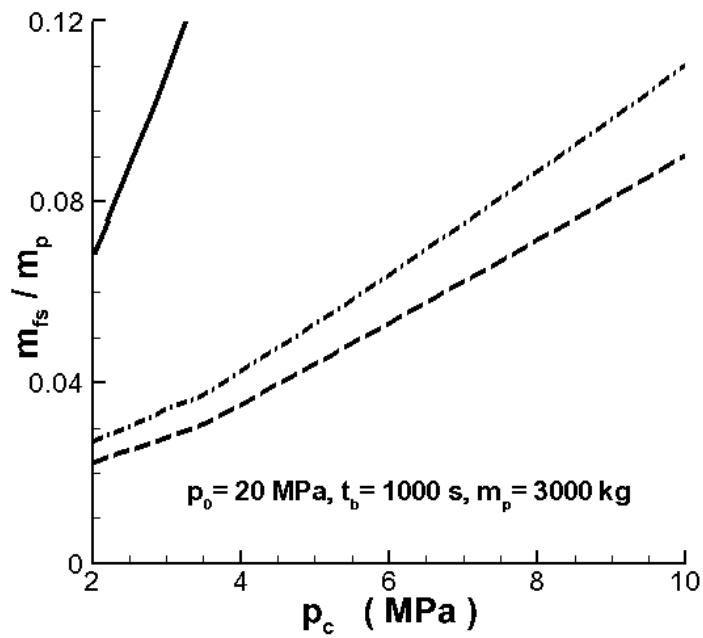
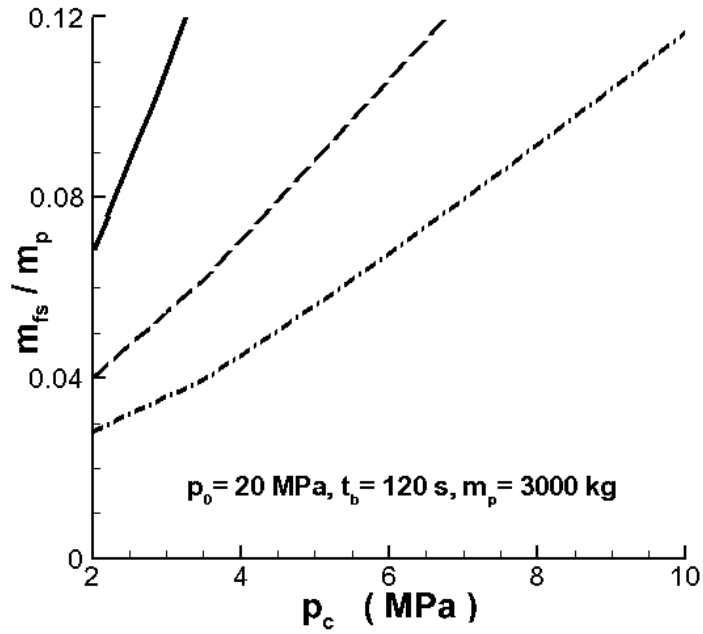


Figure 6:

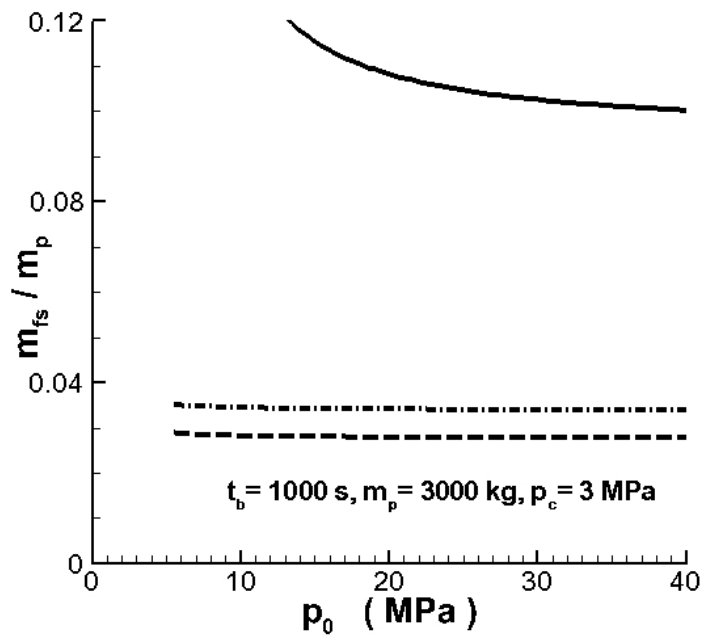
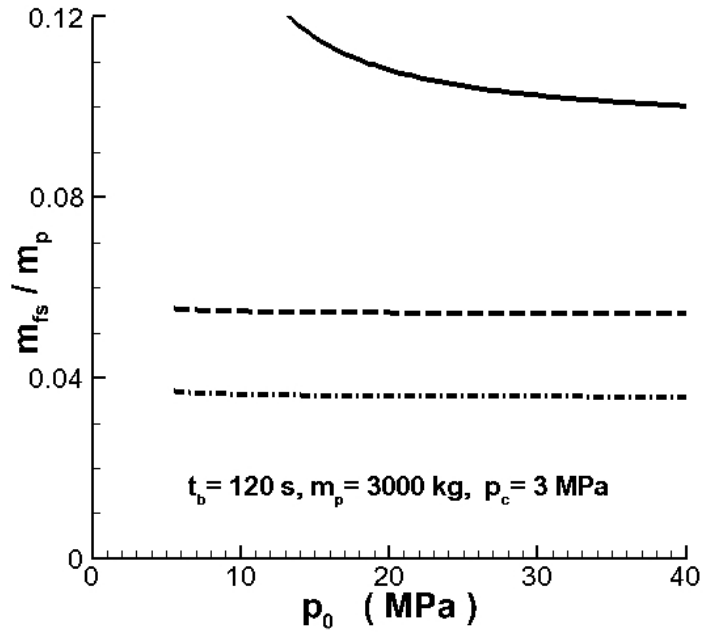


Figure 7:

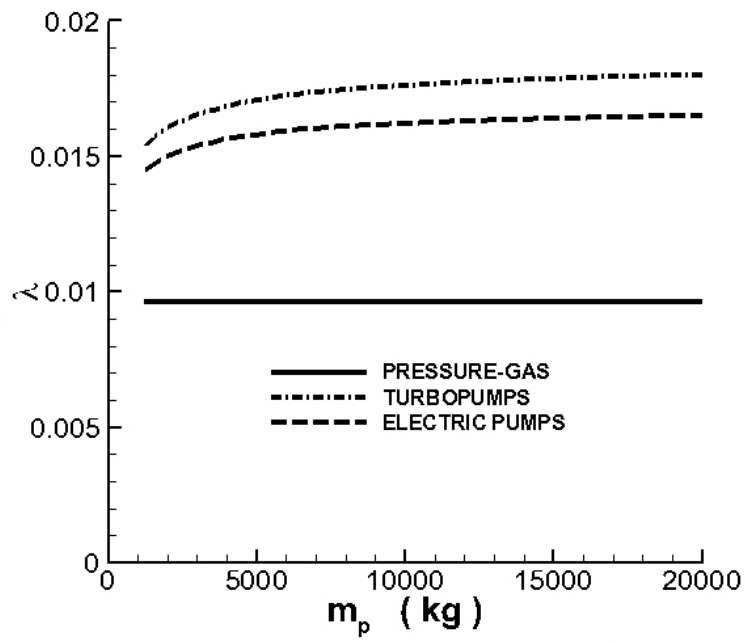


Figure 8:

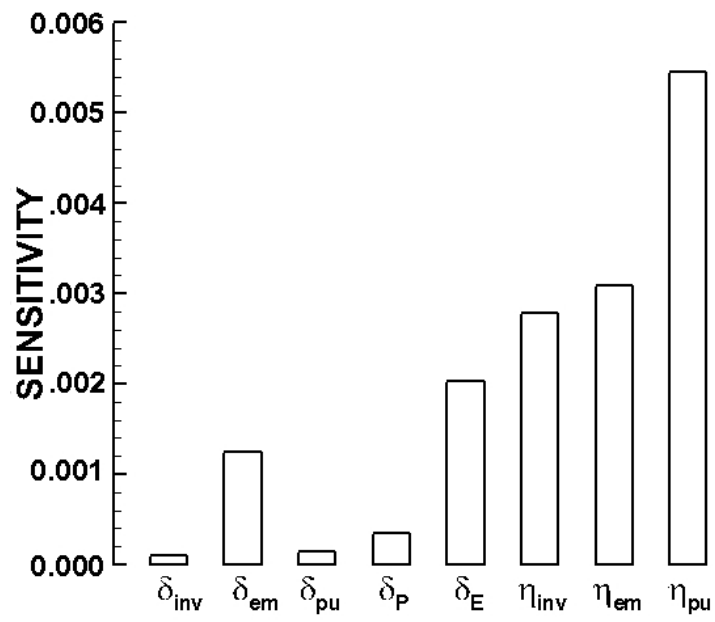


Figure 9: